Tessutivo: Contextual Interactions on Interactive Fabrics with Inductive Sensing

Jun Gong[1], Yu Wu[1,2], Lei Yan[1,3], Teddy Seyed[4], Xing-Dong Yang[1]
Dartmouth College[1], University of Science and Technology of China[2], Beijing University of Posts and Telecommunications[3], University of Calgary[4]
{jun.gong.gr; xing-dong.yang}@dartmouth.edu, teddy.seyed@ucalgary.ca

ABSTRACT

We present Tessutivo, a contact-based inductive sensing technique for contextual interactions on interactive fabrics. Our technique recognizes conductive objects (mainly metallic) that are commonly found in households and workplaces, such as keys, coins, and electronic devices. We built a prototype containing six by six spiral-shaped coils made of conductive thread, sewn onto a four-layer fabric structure. We carefully designed the coil shape parameters to maximize the sensitivity based on a new inductance approximation formula. Through a ten-participant study, we evaluated the performance of our proposed sensing technique across 27 common objects. We yielded 93.9% real-time accuracy for object recognition. We conclude by presenting several applications to demonstrate the unique interactions enabled by our technique.

Author Keywords

Inductive Sensing; Interactive Fabrics; Object Recognition

CSS Concepts

• Human-centered computing - Human computer interaction (HCI);

INTRODUCTION

Input through interactive textiles have found numerous applications in clothing, fashion, furniture, toys, and even vehicles [13, 35, 48, 52]. Thus, it is foreseeable that objects that are already made or covered by soft and lightweight fabrics may become an important part of daily digital life in the near future. However, with current sensing techniques on interactive fabric, user input is limited to either touch [30, 35, 40] or deformation of the fabric [32, 48]. As a result, opportunities for several new interactions techniques have thus been missed.

In this paper, we explore a technique using contact-based inductive sensing for contextual interactions on interactive

fabrics. Our technique is based on the precise detection and recognition of conductive objects (mainly metallic) that are commonly found in households and workplaces, such as keys, coins, and electronic devices. Our technique allows a context embedded object to be sensed by the interactive fabric, when the object is in contact with the fabric. Using this information, a desired application can thus be triggered to respond. For example, a sofa is capable of detecting if a user has left their keys on it after they've left. An empty tablecloth can remind the user to set up eating utensils before guests arrive for dinner. Aside from object recognition, our technique can also sense the coarse movement of the contact area of the object itself, allowing a new dimension of input to be carried out through gestures.

We developed a proof-of-concept prototype (called Tessutivo) to demonstrate technical feasibility and new applications enabled by our technique. Our prototype contains a grid of six by six spiral-shaped coils made of a conductive thread, sewn onto a four-layer fabric structure. The size and shape of the coils were carefully designed to maximize the sensitivity to objects of different materials and shapes. The optimization was performed based on a new mathematical model developed to approximate coil inductance, which is a direct measure of sensor sensitivity. We tested our prototype using 27 common objects that were a mix of conductive objects and non-conductive objects, instrumented using low-cost copper tape. Results from ten participants revealed 93.9% real-time accuracy for object recognition.
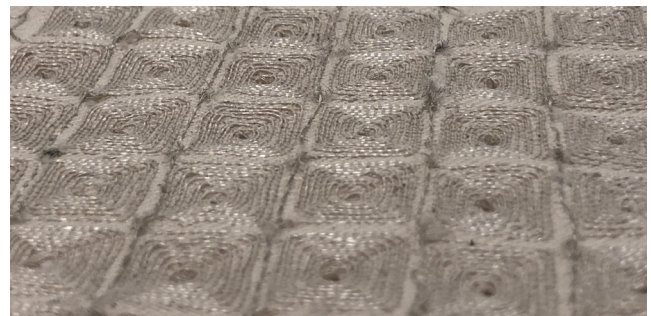

Figure 1. Tessutivo is an interactive fabric that can detect conductive objects placed on it.

Our contributions are: (1) an object recognition technique for interactive textiles that uses inductive sensing; (2) a procedure that can optimize the design of sensor coils to maximize sensitivity; (3) a study evaluating the accuracy our

sensing technique; and (4) several applications to demonstrate the unique interactions enabled by our technique.

RELATED WORK

We briefly discuss prior research into input on interactive fabric, sensing techniques for object recognition, and inductive sensing.

Input on Interactive Fabric

With the current state-of-the-art, user input on interactive fabrics is mainly performed through touch [30, 35, 40] or deforming the fabric itself [32, 48]. The enabling technology behind these innovations can be mainly divided into those using capacitance [26, 34, 35], resistance [20, 30, 31, 40, 52], and optics [13, 45].

The class of work utilizing capacitive sensing is largely based on fabric capacitors made of conductive materials acting as electrode plates. On a piece of fabric, the electrodes can be created using conductive threads or inks. Musical Jacket [34], from MIT exemplifies an early exploration in this field. The authors used stainless steel yarns to embroider a capacitive touch keypad on denim. Meyer et al.'s work [26] describes a multi-layer capacitive textile sensor that can precisely detect input through pressure. A more recent work, Project Jacquard [35], describes the design and fabrication of a new type of conductive yarn that can be woven into textiles using standard looms at scale.

The approaches using resistive sensing are based on fabric resistors. A common structure of the sensor in this category includes two conductor layers separated by a semi-conductive middle layer. eCushion [52] is an example, which has a middle layer made by a semi-conductive material (e.g., yarn coated with piezoelectric polymer) sandwiched by a top and bottom layer made by fabric coated with parallel conductive buses. Applications for this type of sensor are wide. For example, eCushion [52] was developed for detecting sitting postures. GestureSleeve [40] is an interactive sleeve that allows a user to use touch gestures to interact with computing devices on the forearm. proCover [20] uses a similar type of sensor [31] to augment prosthetic limbs. New methods are also being researched to improve resistive sensing technology. For example, Parzer et al.'s method can reduce the sensor layers from three to one via a new type of yarn comprised of a metallic thread with a resistive coating [30].

In the space of interactive fabric, object recognition has been largely overlooked. To the best of our knowledge, the most relevant work is from Rofouei, et al. [37], who proposed to use pressure profiles (e.g., weight and shape) to distinguish objects on a piece of fabric. However, without an evaluation of object recognition on interactive fabric, it is hard to understand how well this technique works. Our inductance-based approach primarily relies on the material of the object and is based on contact not pressure. This allows the sensor to be used in scenarios where weight may not be a reliable indication of an object's identity.

Object Recognition

Within existing research, object recognition can be achieved using two approaches, with the main difference in the need for target objects to be instrumented.

The approach of relying on instrumentation requires the target objects to be tagged. Radio frequency identification (RFID) tag is an example which is used in a large number of object recognition applications [2, 5, 15, 21, 22, 36, 42]. NFC tags is another option, which was used in research projects like Capacitive NFCs [12] and Zanzibar [47]. In the commercial market, optical solutions like QR codes have been widely used to encode information about different products [17]. iCon [8] uses the vision based approach for tangible input through daily objects using pattern stickers. Although instrumenting target objects is generally an effective approach in many application domains, the limitation is obvious as the objects must be tagged, or the technology will not work.

Technologies without the requirement of using tags often rely on computer vision [24], which requires an object to be visible and privacy can be a concern for using cameras [3]. More recently, mechanical or electronic properties of the target objects (e.g., EM signatures, vibration patterns, etc.) are also exploited. For example, acoustics-based approaches (e.g. [33, 50]) recognize objects that can emit a sound. EM-Sense [19] recognizes electrical objects via the electromagnetic signals emitted from the objects. ViBand [18] recognizes objects through patterns of different mechanical vibrations. Radarcat [53] uses multi-channel radar signals to recognize electrical or non-electrical objects. However, object recognition on soft fabric is overlooked.

Sensing Techniques Based on Induction

Inductive sensing has been used in many applications, including position sensing [14, 29, 44] and the detection of defects in metal objects and structures [46]. As for object recognition, Maekawa, et al. [25] used magnetic sensors and coils to recognize electrical objects. Wang, et al. [49] used magneto-inductive sensors to recognize electrical objects via electromagnetic radiation. More recently, ID'em [6] is a tagging method that employed an array of inductive sensors to identify objects instrumented with conductive dots. Indutivo [11] used inductive sensing to enable contact-based, object driven interactions for input-limited devices like smartwatches. Guidelines were provided for the design and implementation of sensors coils to achieve an optimized sensing performance. Our work takes a similar approach but is instead on soft fabric. This imposes many new challenges that only exist on soft fabric. For example, sensor coils are created using conductive threads, which have very different physical and electronic properties than the copper wires used on a rigid substrate. Thus, knowledge developed previously becomes inapplicable to the coil design. We discuss how we

overcame these challenges by generating a new set of knowledge that can be beneficial for future research.

SENSING CONDUCTIVE OBJECTS

Similar to Indutivo [11], Tessutivo can differentiate conductive objects that are either environmental or artificial. Environmentally conductive objects are common in everyday life, from the smartphone to the utensils on a dinner table that sit on a table cloth. Artificial conductive objects are those manually instrumented using conductive markers in the object's contact area (Figure 2). By identifying the unique pattern of the conductive markers through its inductance footprint, the associated object can be recognized. This enabled us to increase the scope of object recognition on an interactive fabric. In this work, we used copper tape to create conductive markers to instrument both conductive and non-conductive objects. Unlike Indutivo [11], whose sensor coils were arranged in a 1D space, our work employs a 2D coil array, thus allowing us to design markers with even richer 2D geometry shapes.
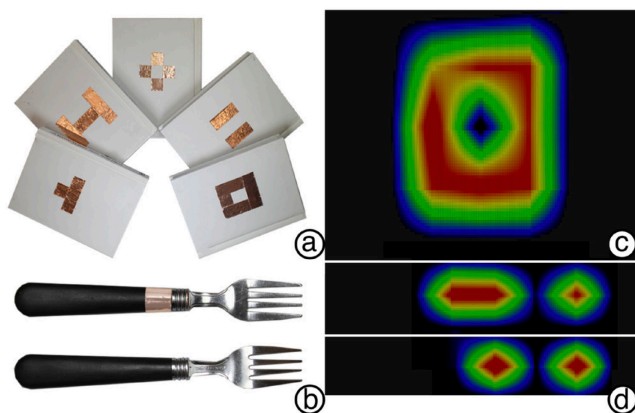

Figure 2. Left: (a) conductive markers created using copper tape. (b) folks with and without instrumentation. Right: (c) heatmap image of inductive footprint of rightmost marker. (d) heatmap images of inductive footprints of the fork and instrumented fork.

SENSING PRINCIPLE

Inductive sensing is a known technology for low-cost, high-resolution sensing of electrically conductive (mostly metallic) objects. Its sensing principle is based on Faraday's law of induction, which can be described as the following: a current-carrying conductor can "induce" a current to flow in a second conductor. For example, when an alternating current (AC) is passed through a L-C resonator, comprising of an inductor (e.g., a *spiral-shaped coil* of the sensor) and a capacitor, it results in a time-varying electromagnetic filed. When a conductive object is brought into this electromagnetic filed, a circulating current known as an eddy current is induced on the surface of the conductive object. In turn, the induced eddy current generates its own electromagnetic field, which opposes the original magnetic field generated by the L-C resonator. Therefore, a shift of the resonant frequency of the L-C resonator can be observed, through a sensor, due to mutual inductance. According to

formula (1), when the resonant frequency changes, the coil inductance changes accordingly. This forms the basis of our sensing technique:

$$f_0 = \frac{1}{2\pi\sqrt{LC}} \tag{1}$$

where f_0 is the measured resonant frequency, L is the coil inductance and C is the capacitance of the known capacitor.

The amount of the change in the resonant frequency or in turn the coil's inductance, relates to an abundance of information about the conductive object, such as its size, shape, electrical properties (e.g., resistivity) and distance. We exploit this information for object recognition. A key component of inductive sensing is the design of the sensor coils, which should aim to reduce the inductance of the coil for improved sensitivity to different objects. This is because when the coil's inductance is small, a tiny change in its inductance caused by a target object can be related to a more observable shift in the measured resonant frequency [11].

Most conductive objects have capacitance and inductance, and both properties affect the resonant frequency. The effect of inductance dominates that of capacitance with most metallic objects. In contrast, the effect of capacitance becomes dominant with most non-metallic conductive objects, such as a finger. As a side effect, our system can also differentiate a finger from conductive objects due to the opposing influence on measured resonant frequency from both effects.

FABRICATING SENSOR COIL

Unlike the existing work [6, 11], where the sensor coils were printed on a rigid substrate, developing inductive sensing on a textile requires a different approach. We used conductive threads, which can be easily stitched on a fabric to spiral the coils using a home embroidery sewing machine (e.g., Brother SE600). In comparison to other options like printing [16], stitching creates traces that are mechanically stable and durable [10]. The shape patterns of the coils (e.g., shape and size) can be designed using graphics editing software (e.g., Microsoft Paint, Adobe Illustrator) and then saved into the embroidery file format using SewArt Embroidery Digitizer. This approach is simple and easy, even for novice makers.

Two layers of coils is also possible by aligning two single layer coils back-to-back. However, this is not easy because the standard stitching process on a sewing machine pushes the conductive threads through the substrate, causing short circuits between the opposite-side coils. We overcame this challenge by adopting the method discussed in Dunne et. al.'s work [10]. We carefully tuned the tension of the top thread (e.g., non-conductive thread) to ensure that the conductive thread on the back only floated on the surface of the substrate without penetrating it. We then sewed the two layers together, with the coils well aligned, facing outwards. Finally, the opposite-sided coils need to be connected. This was done by connecting the spiral center together using twist splice. The connection was then fixed in place using a touch

of hot glue for the sake of simplicity or the glue can be replaced using stitch. The coil layers are then sandwiched between two insulation layers to avoid the coils to be shorted by the conductive object (Figure 3).
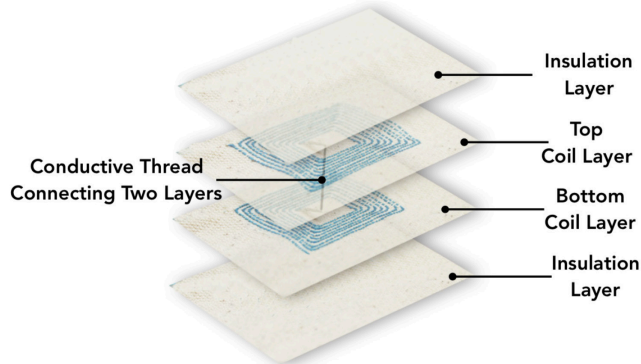

Figure 3. The four layer-combination of Tessutivo.

CONDUCTIVE THREAD OPTIONS

One of the major challenges in enabling inductive sensing on a soft fabric is the choice of the right conductive threads. First, the threads should guarantee a high conductivity, otherwise the self-resonant frequency of the coil may decrease to a level that intersects with the resonant frequency of the sensor (e.g., L-C resonator) [10]. This will cause serious jittering in the sensor signal, as we discuss later in this section. Second, the conductive thread should be thin. This is because thick threads are hard to sew using a standard home sewing machine up to the level of precision needed to make the coils. Amongst what is available on the market currently, only 4 candidates satisfied our needs (shown in Table 1), within which, all threads are made of stainless steel, except for the LIBERATOR 40, which is made of silver-plated fiber. The conductivity of these candidates ranges from 3.28 to 91.84 Ω/m (e.g., all below 100 Ω/m). Although these threads are significantly more conductive than other threads which are available commercially, we were still unsure about whether they were good enough for our needs, as existing literature provided us with little insight into the conductivity requirement for the creation of sensor coils using conductive threads.

Name	LIBERATOR 40	Stainless thin thread	Smooth conductive thread	Conductive thread bobbin
Manuf. /Distributor	Syscom	Adafruit	Sparkfun	Sparkfun
Yarn Type	Single twine	Double twine	Triple twine	Double twine
Material	Silver coated polymer	316L Stainless steel fiber	12UM Stainless steel fiber	316L Stainless steel fiber
Thickness (mm)	0.18	0.20	0.12	0.35
Conductivity (Ω per m)	3.28	51.18	27.00	91.84

Table 1. Conductive Yarn Candidates.

Thus, we conducted an experiment to test the signal stability of these different thread options (Figure 4). In our experiment, we used each of these threads to create a rectangular-shape coil (e.g., $d_{out} = 30mm, n = 10, s = 0.90mm$, see parameter descriptions later) using a sewing and embroidery machine (Brother SE600). As we were only interested in knowing the effect of the thread material, we did not optimize the shape parameters of the coils in this test (discussed later). The substrate used in this test across all the thread options was Drill 40 Unbleached 17181 (100% cotton). The signals from the tested coils were measured using a Texas Instruments LDC1614 evaluation board for inductive sensing. We used software (i.e. Sensing Solutions EVM GUI) alongside the evaluation board to acquire sensor signal (e.g., sensor's inductance).

Our results revealed that only the LIBERATOR 40 was conductive enough to guarantee the stability of sensor signal. The sensor inductance measured from the stainless-steel threads were all extremely jittery. The highest variance observed reached up to ~1000uH, even without the presence of a conductive object. This was significantly higher than the normal range of 0.002uH, observed from the coils made of LIBERATOR 40. As discussed earlier, the jittering is mainly due to the lack of conductivity of the sensor coils. Therefore, we chose the LIBERATOR 40 for our sensor development. LIBERATOR 40 has a light-weight, flexible and high-strength fiber core with a conductive metal outer layer, which is commonly used as shielding braid, bare wire, or is coated with insulation material.
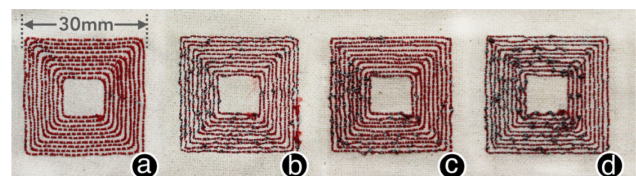

Figure 4. Four tested coils made of different conductive threads: (a) LIBERATOR 40, (b) Stainless thin thread, (c) Smooth conductive thread, and (d) Conductive Thread Bobbin.

COIL DESIGN

This section discusses (in several dimensions) how the design of sensor coils can be optimized around coil inductance in the context of interactive fabric.

Coil Size and Layer

As mentioned in the *Sensing Principle* section, our goal was to reduce coil inductance to improve the sensitivity of the sensor to different objects. In practice however, the minimum coil inductance is bound by the working range of the inductance-to-digital converter. For example, the LDC1614 chip has a lower bound at around 1.49uH with suggested 680pF capacitor (or 5MHz in resonant frequency), below which sensor signals become unstable (as suggested by [11]). Therefore, the most suitable coil design for us is one that has a coil inductance of around 1.49uH, but not smaller.

Aside from coil inductance, our application has a constraint in the size of the coil as a small and dense grid of coils

enables a greater sensing resolution in a 2D space, for both detecting object movements on the fabric surface, as well as sensing the shape of the object's contact area, which is useful for gestural input using a conductive object. Therefore, our goal was to design the coil to be the smallest in size without violating the inductance requirement.

Once we achieved these goals, coil size can be further reduced without decreasing coil inductance using a multi-layer design (e.g., 2, 4, 6 layers). Therefore, in this work, we used a two-layer design. Although more layers are possible, we considered two to avoid the fabric to be too thick. Finally, optimizing the other parameters can help further minimize coil size without reducing coil inductance.

Coil Shape

In principle, a coil can be made into any shape, but the most common ones are square, hexagon, octagon, and circle (Figure 5). The shape of a coil mainly affects sensing distance and sensing area. The circular shape has the best quality factor and lowest series resistance [1], thus allowing the largest possible sensing distance among the four options [27]. Alternatively, a rectangular shape has the largest sensing area per coil unit in a 2D space. For our application, sensing distance should be kept small to avoid false positives while the sensing area should be kept large to maximize sensing region. We thus used the rectangular shape for our sensor.
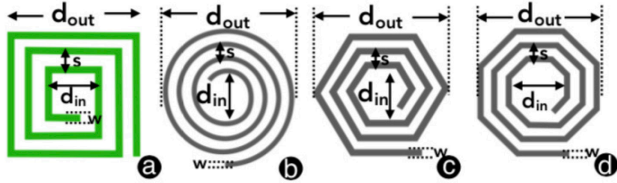

Figure 5. Four common designs of planar spiral coil: (a) square, (b) circle, (c) hexagon, and (d) octagon. d_{out} and d_{in} are outer and inner diameters respectively.

Coil Shape Parameters

Once the shape is determined, the shape parameters need to be optimized to achieve the desired inductance.

For a given shape, a coil can completely be specified by the number of turns (n), width of trace (w), trace spacing (s), and any one of the following: the outer diameter d_{out}, the inner diameter d_{in}, the average diameter, defined as $d_{avg} = (d_{out} + d_{in})/2$ and the fill ratio, defined as $\rho = (d_{out} - d_{in})/(d_{out} + d_{in})$ (Figure 5)

If the value of each shape parameter is determined, the coil inductance can be calculated in theory using the sheet approximation formula [38]. However, the challenge here was that this formula was designed for coils made from copper and does not work for silver plated fiber, whose electronic properties vary significantly. Therefore, we constructed our own formula. We did so by using curve fitting, similar to a previously used approach [28].

Inductance approximation formula for single-layer coils
For the single-layer design, we used the monomial fitted inductance equation proposed by Mohan et al. [28]:

$$L_{single} = \beta d_{out}^{\alpha_1} w^{\alpha_2} d_{avg}^{\alpha_3} n^{\alpha_4} s^{\alpha_5} \qquad (2)$$

where L_{single} is the inductance of the coil of a certain design, which can be measured using an LCR Meter; w is a constant value indicating the width of the conductive thread (e.g., 0.18mm for LIBERATOR 40); β and α_i are unknown coefficients specific to the LIBERATOR 40 thread. Their values were determined by identifying the best fit to the measured inductance values of a set of known coil designs.

To capture data for curve fitting, we used five different values for d_{out}, ranging from 10mm to 30mm, with a constant interval of 5mm. We also used five different values for spacing s, ranging from 0.54mm ($3 \times w$) to 0.90mm (5 $\times w$), with an interval of 0.09mm ($0.5 \times w$). Note that the typical spiral coils are built with $s \leq w$ to maximize the interwinding magnetic coupling [28]. However, this is extremely hard to achieve on a fabric using stitching. Therefore, s started from 0.54mm ($3 \times w$) in our study.

As suggested by [28], we iterated all possible numbers of turns (n) that could lead to the coil designs satisfying the requirements of $0.1 \leq d_{in}/d_{out} \leq 0.9$. Note that the relationship between number of turns (n) and d_{in} can be determined using the following formula.

$$d_{in} = d_{out} - 2(n-1)(w+s) - 2w \qquad (3)$$

In total, we came up with 229 different coil designs for data fitting, each representing a $d_{out} \times s \times n$ combination. We stitched the coils on the Drill 40 substrate using the Brother sewing machine. The inductance (L_{single}) of each design was measured manually using a DE-5000 Handheld LCR Meter.

A logarithmic transformation was used on both sides of the equation (4), before a least squares fitting was used to fit the data. The resulting approximation formula is:

$$L_{single} = 0.001 \cdot d_{out}^{-0.7} d_{avg}^{2} n^{1.7} s^{-0.2} \qquad (4)$$

The R-squared and root-mean-square error for this model is 0.995 and 0.088 respectively, indicating that the model fits the testing data well.

Inductance approximation formula for multi-layer coils
In a multi-layer design, the total inductance (L_{total}) of the coils in series (e.g., the two opposite-side coils), can be calculated using formula (5) [39].

$$L_{total} = \sum_{i=1}^{N} L_i + 2 \cdot (\sum_{j=1}^{N-1} \sum_{m=j+1}^{N} M_{j,m}) \qquad (5)$$

where N is the number of layers (2 in this case). $M_{j,m}$ is the mutual inductance between the coils, which is defined as $k \cdot \sqrt{L_j \cdot L_m}$, in which, L_j and L_m are the inductance of layer j and m, which can be calculated using equation (4). The parameter k is the measure of the flux linkage between the coils, whose value varies between 0 and 1. According to

Zhao's work [54], k is only related to number of turns (n) and a relative constant thickness of the fabric substrate (e.g., 1mm in the case of two Drill 40 substrates). Thus, k can be described using the following formula:

$$k = \gamma \cdot \frac{n^2}{0.64*(1.67n^2 - 5.84n + 65)} \quad (6)$$

where γ is the unknown coefficient, which could also be found using a least squares fitting. Within the 229 coil designs we used to find the equation for the single-layer coils, and for each possible n (e.g., from 2 to 19), we chose those with the largest, smallest and medium inductances, which were then stitched into two Drill 40 substrates and sewn together. The inductance L_{total} of each design was measured manually using a DE-5000 Handheld LCR Meter. After fitting, the resulting approximation formula for a two-layer design is shown in Formula (7) with:

$$L_{total} = L_1 + L_2 + \frac{2.27n^2}{0.64*(1.67n^2 - 5.84n + 65)} \cdot \sqrt{L_1 L_2} \quad (7)$$

The R-squared and root-mean-square error for this model is 0.992 and 0.49 respectively, indicating that the model fits the testing data well. We used this model to guide the optimization of our final coil designs.

Final Coil Design
With formula (7), our goal was to traverse all 7165 possible design solutions, calculate the theoretical inductance value for each candidate, and narrow down the search by identifying the smallest coils with an inductance of around 1.49uH. Table 2 shows the finalist.

Outer Diameter (mm)	Trace Spacing (mm)	Turns	Approx. Inductance (uH)	Real Inductance (uH)	Real Resonant Frequency (MHz)
13	0.54	8	1.605	1.507	4.972
13	0.55	8	1.572	1.475	5.025
13	0.56	8	1.539	1.428	5.107

Table 2. Coil designs that satisfied our needs. The one highlighted in the first row was chosen.

We implemented all candidates in our shortlist by stitching them on the Drill 40 substrate. The inductance values of the designs were measured using the LCR meter. Our result revealed that the inductance of all the candidates in the shortlist were around 1.49uH but only one had a value higher than 1.49uH, which satisfied our requirement. This suggests that our model is mostly effective but still lacks in precision, which was expected. Figure 6 shows the final coil design developed in our prototype.

THE EFFECT OF FABRIC SUBSTRATES
Before we implemented our prototype, we conducted a preliminary evaluation to understand if the material of the fabric substrates has an effect on a coil's inductance. Since the effect of the thickness of the substrates is known, this experiment only focused on the material. This is why we used a single-layer version of the sensor. Among the numerous options available in the market, we chose six representatives made from polyester, lyocell, nylon, modal

rayon, Bemberg rayon, and cotton, as they are commonly used in garments, toys and furniture (Table 3).

Name	Lp Satin Solid Black 17120	Dark Wash 17330	Ripstop 18189	White Modal 16360	Black Ambience 18081	Drill 40 Unbleached 17181
Manuf.	Glitterbug	DENIM	Utility Fabric	DENIM	Lining	Utility Fabric
Material	100% Polyester	100% Lyocell	100% Nylon	100% Modal Rayon	100% Bemberg Rayon	100% Cotton
Average Inductance (uH)	0.478 (s.e.= 0.009)	0.479 (s.e.= 0.022)	0.455 (s.e.= 0.024)	0.473 (s.e.= 0.020)	0.456 (s.e.= 0.016)	0.460 (s.e.= 0.006)

Table 3. Different types of substrates we tested in the study.

We used our final coil design in single layer and stitched five coils on each tested substrates (Figure 6). We then measured inductance of the 25 sensors using the LDC1614 evaluation board. There was no observable difference between the average sensor data obtained from the five substrates, which suggested that substrate material had a neglectable effect on sensor signal (Table 3). For our prototype, we chose the Drill 40 Unbleached 17181 (100% cotton) due to the wide adoption of cotton in fabric materials and relatively small variance [9].
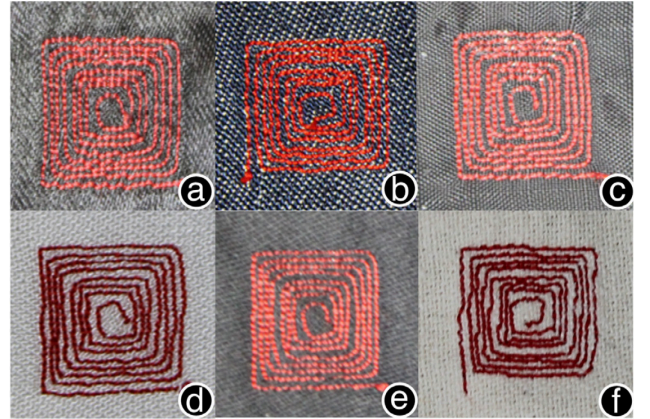

Figure 6. Coils on the six different types of substrates: (a) Polyester, (b) Lyocell, (c) Nylon, (d) Modal Rayon, (e) Bemberg Rayon, and (f) Cotton.

CUSTOMIZED SENSING BOARD
We built our customized sensing board (Figure 7) using a Cortex M4 micro-controller (MK20DX256VLH7) powered by Teensy 3.2 firmware. The board has four 4:1 multiplexers (FSUSB74, ON Semiconductor), an inductive sensing chip (LDC1614, Texas Instruments), a power management circuit, and a Bluetooth module (RN42, Microchip Technology). The sensing board can now drive at most 8×8 coils. We used two multiplexers to control the columns of the coils and another two to control the rows. Our prototype employed a 6×6 grid layout of coils (Figure 7).

Note that we did not use a multiplexer with more input channels (e.g., 8:1 or 16:1). This is because there is a side effect of having extra input channels - increased on-resistance (R_{on}) and on-capacitance (C_{on}), which may cause

serious jittering in the sensor's signal. Our initial test suggested that in order for the LDC1614 to work properly, R_{on} and C_{on} should be less than 10 Ω and 10 pF respectively. Among what is available commercially, few products satisfy this requirement. We thus decided to use a 4:1 multiplexer instead. R_{on} and C_{on} of our multiplexers is 6.5 Ω and 7.5 pF respectively.

The system has a sampling rate of around 300 Hz. All sensor readings were sent to a Macbook Pro laptop for data processing via Bluetooth. In total, the entire system consumes 250.5mW of power, including those consumed by the Bluetooth radio (99mW). With a 650mAh lithium-polymer battery, the system can work for at least 2 hours.
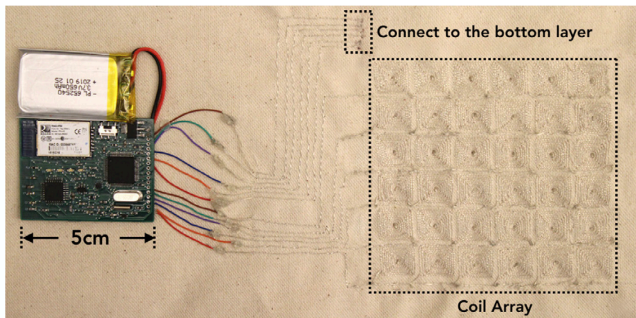

Figure 7. Tessutivo prototype and sensing board.

WIRE CONNECTION
The next challenge is to connect the coils to our sensing board. Connecting the conductive threads to rigid electronics is currently an open problem yet to be solved [30, 35]. A number of methods were used in previous research, which include using snap buttons, sewing, conductive epoxy, crimping and so on [4, 32, 35, 40]. In the case of LIBERATOR 40, the thread can be soldered directly under a certain temperature by following its datasheet. However, our tests found that solder heat made the tip of the thread (at its connection) extremely fragile, causing unreliable wire connections across the sensor grid. After iterating upon a number of different methods, such as snap buttons, we found the most effective and reliable method to connect the thread to an electric wire, was to use a splice shown in Figure 8. It was robust against stretching and folding. Once all the threads were connected to the electric wires, the connections needed to be fixed in place. We used a touch of hot glue in our implementation. Although a bit bulky in its current form, this type of connection was stable, durable, and performed well in our final experiment.
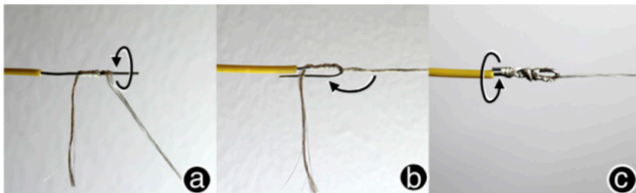

Figure 8. Splice used to connect a conductive thread to a wire.

OBJECT RECOGNITION
Our system recognizes a conductive object by comparing its inductance footprint with a machine learning model trained using a pre-collected database of labeled references. In this section, we discuss our object classification pipeline.

Data Processing
When a conductive object is placed anywhere inside the sensor, the sensor reports a 6 × 6 array of inductance values, one from each coil. This data contains the 2D inductance footprint of the object, describing object material (e.g., resistivity) and low-resolution geometry information of the object's contact area.

Before object recognition is performed, the raw sensor data from each coil was smoothed using a low pass filter to reduce the fluctuations in sensor readings. The data was then mapped to a value from 0 to 255 using the peak value observed from each coil. Finally, we upscaled the sensor data from 6 × 6 pixels to a 100 × 100 heatmap image using linear interpolation. Figure 9 demonstrates an example of a Coke can and its corresponding inductance footprint shown in a heatmap image.
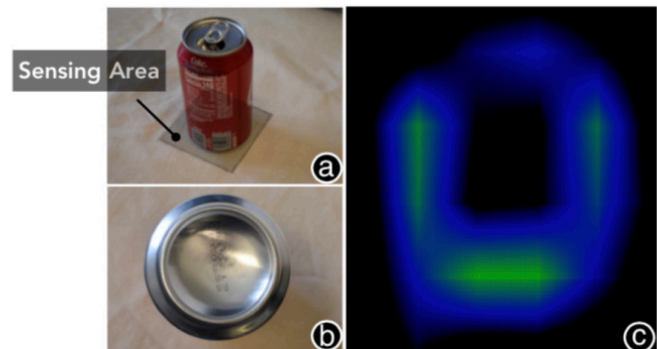
Figure 9. The heatmap image of the inductance footprint of a Coke can.

Machine Learning
We used machine learning for object recognition. While there are many options for classification algorithms (e.g., Hidden Markov Models and Convolutional Neural Networks), many of them are computationally expensive, and thus were considered less suitable for real-time applications in low-power embedded platforms, like wearables [23]. In our implementation, we used Random Forest because it has been found to be accurate, robust, scalable, and efficient in applications involving small devices [7, 41, 43].

Feature Extraction
Object recognition using inductive sensing is primarily based on two types of information, the material and 2D geometry of the contact area of the objects. Based on our observation and initial tests, we derived 81 features, shown in Table 4. We selected the features that are invariant to the location and orientation of the contact area of the object.

Figure 10. The tested conductive objects. (A) candy box, (B) binder clip, (C) travel mug, (D) tip tinner box, (E) coil, (F) finger, (G) folk, (H) Coke can, (I) metal credit card, (J) spoon, (K) USB drive, (L) k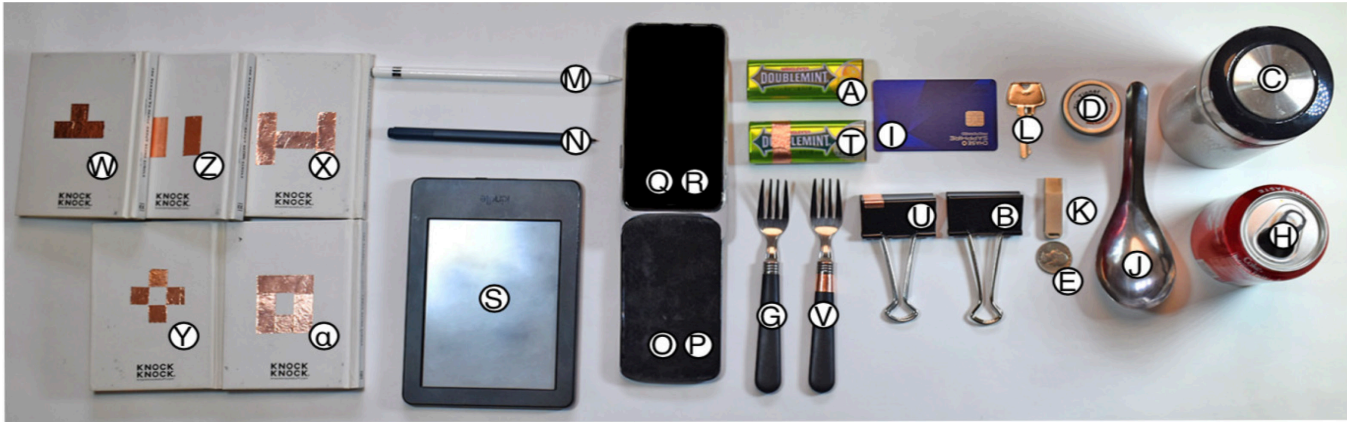ey, (M) Apple pen, (N) Surface pen, (O) Nexus 4 front, (P) Nexus 4 back, (Q) iPhone X front, (R) iPhone X back, (S) Kindle, (T) instrumented candy box, (U) instrumented binder clip, (V) instrumented folk, (W-Z, α) instrumented books.

Finger Detection

With the presence of the finger, the inductance readings measured by the sensor increases slightly instead of decreasing due to the capacitance effect discussed before. So, we used a simple heuristic to identify the finger by checking whether sensor readings surpass a threshold chosen by a pre-test.

Shape-Related Features (49 features)	• **Local Binary Pattern (36)** • **Hu Moments (7)** • **Object Area (1):** Number of pixels the object covers • **Object Edge (1):** Number of pixels the object's edge covers • **Average Distance (4):** Average distance from object's pixels to object's center of gravity and geometric center (2), Average distance from object's edge pixels to object's center of gravity and geometric center (2)
Material-Related Features (32 features)	• **Statistical Functions (11):** Mean, Variance, Max, Local Maximum Numbers, Median, Quantiles (3), Count above/below mean, Absolute Energy of the object's pixel values • **Entropy (1):** Binned Entropy • **Ten-Fold Stats (20):** Sort and divide the object's pixel values into 10 folds and average for each fold (10), Divide grayscale values (e.g., 0~255) into ten intervals and count the number of the pixels in each interval (10)

Table 4. The feature set we extracted to train our ML model.

SYSTEM EVALUATION

We conducted an experiment to evaluate the performance of Tessutivo. The goal was to validate the object recognition accuracy of our prototype. We were also interested in evaluating sensor robustness against individual variance among different users.

Participants

10 right-handed participants (average age: 23, 8 males, 2 females) were recruited to participate in this study.

Objects

We tested our prototype using 27 common conductive objects in households and workplaces to encompass a broad range of different properties (e.g., size, material, shape). The objects can be classified into four types: *large* or *small* objects and *instrumented conductive* or *instrumented non-conductive* objects (Figure 10). Large objects had a contact area greater than the active sensing region of our system (e.g., the 6 × 6 grid). Some of were metallic, while others were electronic devices with built-in metallic components. Small objects had a contact area smaller than the sensing area. Instrumented conductive objects are those with a contact area instrumented using copper tape of 13 mm wide. Instrumented non-conductive objects are non-conductive objects with the contact areas instrumented using copper tape with different patterns.

Study Procedure

Three days prior to our study, training data was collected by a volunteer with the sensor that was powered by a wall outlet (earth ground). The sensor was put on a rigid table and a volunteer was asked to place an object on the sensor in random orientations and locations inside the sensing area. The only instruction the volunteer was given was to ensure the object's contact area to be exposed to the sensor as much as possible. Sample data was collected 30 times per object. This volunteer was excluded from our final study.

Prior to the start of the final study, participants learned tested objects and they also understood that the object's contact area needed to be exposed to the sensor as much as possible. No other instruction or practice trial was given. The study protocol was similar to the one used in [18, 51], where a live object recognition study was carried out with 27 objects. Unlike putting the sensor on a rigid table in the training phase, participants were asked to place the tested objects on the seat of a sofa, instrumented with our prototype. We deliberately designed this procedure to evaluate how our collected object model worked in a more realistic setting, as

daily objects that are made or covered by fabrics are commonly soft (e.g., sofa, clothing, toys).

Result

Overall, an accuracy of 93.9% (s.e. = 0.69%) was achieved by our system. Figure 11 describes the confusion matrix for all objects described previously. Among the 27 tested objects, 24 objects achieved an accuracy higher than 90%. This is a promising result, as we purposefully included typical experimental procedures that impact recognition accuracy – no user training, no per-user calibration, large time gap between training data collection and the study itself. The confusion matrix revealed that the candy box was occasionally misclassified as a 5cm binder clip. This occurs when two objects are of a similar material (e.g., steel) are compared. This is further emphasized, when the contact area appears similar under the resolution of our current grid implementations.

	A	B	C	D	E	F	G	H	I	J	K	L	M	N	O	P	Q	R	S	T	U	V	W	X	Y	Z	α
A	90	6	0	0	0	0	0	0	0	0	0	0	0	0	0	0	0	0	0	4	0	0	0	0	0	0	0
B	6	94	0	0	0	0	0	0	0	0	0	0	0	0	0	0	0	0	0	0	0	0	0	0	0	0	0
C	0	0	90	4	0	0	0	6	0	0	0	0	0	0	0	0	0	0	0	0	0	0	0	0	0	0	0
D	0	0	4	96	0	0	0	0	0	0	0	0	0	0	0	0	0	0	0	0	0	0	0	0	0	0	0
E	0	0	0	0	100	0	0	0	0	0	0	0	0	0	0	0	0	0	0	0	0	0	0	0	0	0	0
F	0	0	0	0	0	100	0	0	0	0	0	0	0	0	0	0	0	0	0	0	0	0	0	0	0	0	0
G	0	0	0	0	0	0	94	0	0	2	0	0	0	0	0	0	0	0	0	4	0	0	0	0	0	0	0
H	0	0	6	0	0	0	0	94	0	0	0	0	0	0	0	0	0	0	0	0	0	0	0	0	0	0	0
I	0	0	0	0	0	0	0	0	90	0	0	0	0	0	4	6	0	0	0	0	0	0	0	0	0	0	0
J	0	0	0	0	0	0	0	0	0	94	2	4	0	0	0	0	0	0	0	0	0	0	0	0	0	0	0
K	0	0	0	0	0	0	0	0	0	0	96	4	0	0	0	0	0	0	0	0	0	0	0	0	0	0	0
L	0	0	0	0	0	0	0	0	8	4	88	0	0	0	0	0	0	0	0	0	0	0	0	0	0	0	0
M	0	0	0	0	0	0	4	0	0	0	0	0	96	0	0	0	0	0	0	0	0	0	0	0	0	0	0
N	0	0	0	0	0	0	4	0	0	0	0	0	0	96	0	0	0	0	0	0	0	0	0	0	0	0	0
O	0	0	0	0	0	0	0	0	0	0	0	0	0	0	96	4	0	0	0	0	0	0	0	0	0	0	0
P	0	0	0	0	0	0	0	0	0	0	0	0	0	0	0	96	0	4	0	0	0	0	0	0	0	0	0
Q	0	0	0	0	0	0	0	0	0	0	0	0	0	0	0	6	94	0	0	0	0	0	0	0	0	0	0
R	0	0	0	0	0	0	4	0	0	0	0	0	0	0	0	0	8	88	0	0	0	0	0	0	0	0	0
S	2	0	0	0	0	0	0	0	0	0	0	0	0	0	0	2	0	2	94	0	0	0	0	0	0	0	0
T	10	2	0	0	0	0	0	0	0	0	0	0	0	0	0	0	0	0	0	88	0	0	0	0	0	0	0
U	2	6	0	0	0	0	0	0	0	0	0	0	0	0	0	0	0	0	0	0	92	0	0	0	0	0	0
V	0	0	0	0	0	0	0	0	0	0	0	0	0	0	0	0	0	0	0	0	0	98	2	0	0	0	0
W	0	0	0	0	0	0	4	0	6	0	0	0	0	0	0	0	0	0	0	0	0	0	90	0	0	0	0
X	0	0	0	0	0	0	0	0	0	0	0	0	0	0	0	0	0	0	0	2	0	0	0	94	2	0	2
Y	0	0	0	0	0	0	0	0	0	0	0	0	0	0	0	0	0	0	0	0	0	0	0	0	100	0	0
Z	0	0	0	0	0	0	0	0	0	0	0	0	0	0	0	0	0	0	0	0	0	0	0	2	96	2
α	0	0	0	4	0	0	0	0	0	0	0	0	0	0	0	0	0	0	0	0	0	0	0	2	0	2	92

Figure 11. Object confusion matrices across 10 participants. Results are shown in percentage.

It is exciting to see our system could classify an Apple Pen and a Surface Pen with a high accuracy (e.g., 98%), as these two objects share very similar contact areas but different in the electronics. It shows that our system could effectively distinguish objects with a similar shape but made of different materials. The instrumented non-conductive objects were not significantly confused with each other, indicating that the system could separate them only using the conductive patterns. Keys achieved the lowest accuracy (e.g., 86%) among all objects, as it was primarily confused with the spoon and USB drive. For some of these objects with a small contact area, the system could not reliably identify them because their inductance footprints appeared to be similar to each other again due to the relatively low resolution of our coil grid. The back of an iPhone X was also confused with the back of a Nexus 4. This is because both objects have a similar inner structure with electronics and PCBs.

DEMO APPLICATIONS

We propose four application examples on (1) a tablecloth, (2) in a pocket and (3) a backpack, to showcase possibilities and demonstrate Tessutivo's sensing capabilities.

The first application is a hydration tracker, which reminds a user of their daily water consumption when they are working at a desk. Placing a stainless mug (which we use to track) on a tablecloth starts a timer and a reminder is sent to the user's phone if the mug stays at the desk longer than a pre-set time period (Figure 12 a).

The second application relies on a pocket that is instrumented with Tessutivo. The pocket is capable of detecting if a user's phone has slipped out of the pocket when they have gotten up and left from a sofa (Figure 12 b).

Our third application combines the tablecloth and a backpack to provide unobtrusive contextual sensing. For example, when a user wants to read an ebook, they grab a kindle from a table, which causes the nearby floor lamp to switch on. After the user finishes reading and puts the kindle into their backpack, the lamp turns off automatically (Figure 12 c).

Finally, our last application is also based on a tablecloth in a dining room. A family meal has been prepared by a mother and father, whom have finished cooking and are preparing the table. As they prepare the table, their children whom are on the second floor receive a message asking them to go downstairs and enjoy the meal (Figure 12 d).
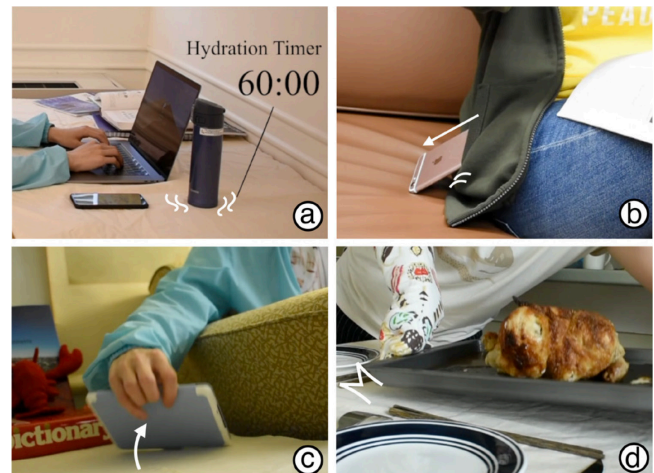
Figure 12. Tessutivo demo applications.

LIMITATIONS AND FUTURE WORK

In this section, we discuss the lessons and insights we learned from our experience. We also present limitations of our work and directions for future research.

Inductance Formula. Our coil inductance estimation formula was derived based on LIBERATOR 40 with the goal of demonstrating the feasibility of inductive sensing on a soft fabric. Further investigation is currently underway to evaluate how well the derived formulas perform with other types of conductive threads. Therefore, our main contribution of this work is not the model. Rather, we see the procedure in the design and implementation of Tessutivo being the contribution that can be generalized beyond the present work and can provide useful guidance for future research in related fields.

Fabric Losing Flexibility. The presented research optimized the coil based on size and sensitivity. We see it a fruitful research direction in the future to consider other parameters. Preserving the softness of the fabric substrate can be one important consideration in future explorations. With our current implementation, the threads are spiraled tightly inside a small area of the coil, which has made the substrate harder than it was before instrumentation. There is a tradeoff between the size of the coil and how well we can preserve the softness of fabric substrate. A larger coil with the threads loosely spiraled inside it may lead to an increase in softness but sensing resolution may decrease.

False Detections upon Sensor Deformation. Sensor readings can be affected if the coil is deformed, which may consequently introduce false detections. Although, our lab study revealed no significant effect of deformation in recognizing the tested objects, we are planning to test Tessutivo in different usage applications and scenarios, such as jean pocket to investigate how robust the system can perform in a more realistic setting and identify areas for improvement.

Contact Area. Objects are required to be in contact with the sensor for our current implementation. Consequently, it can be extremely challenging for detection of objects that don't have a planar contact surface, as inductance values may change as the contact area changes. However, this challenge can be overcome with additional training data since the change in the inductance is consistent with respect to how the object's contact area may change.

Sensing Non-conductive Objects. Our method does not work with non-conductive objects without instrumentation. This is a limitation of the induction-based approach. A hybrid approach integrating inductive sensing with the other types of sensing techniques, such as those based on pressure, is an interesting future direction to explore. Another possible direction to explore is examining how to make it easier for users to design, fabricate and instrument unique conductive markers on non-conductive objects.

Content Inference. Some of the conductive objects might be containers (e.g., travel mug). A careful evaluation is necessary in the future for investigating the effect of the content within the container (e.g., water or coke).

Finger Detection and Capacitive Sensing. Our current system only uses a simple heuristic to identify a finger, which may introduce false positives in real world settings. However, we believe that a machine learning based model can further improve the robustness. It is also interesting to further explore capacitive image sensing using Tessutivo, which may open up a broader interaction and application space.

CONCLUSION

This paper presents a contact-based inductive sensing approach on interactive fabrics to recognize daily conductive objects. We discuss the sensing principle and our investigation on different conductive threads and substrates. We built a prototype with a six by six coil array, which was carefully designed to maximize the sensitivity to conductive objects based on an approximate inductance formula derived for conductive thread. Through a ten-participant user study, we demonstrated that our approach yielded a 93.9% real-time classification accuracy with 27 daily objects that included both conductive and non-conductive objects instrumented using low-cost copper tape. Our work presents a novel sensing methodology for object recognition on interactive fabrics. We believe it holds the potential to further enlarge the input space of interactive fabrics.

REFERENCE
[1]   TI LDC Sensor Design Application Report SNOA930. 2015. Retrieved March 15, 2019 from http://www.ti.com/lit/an/snoa930a/snoa930a.pdf

[2]   Eugen Berlin, Jun Liu, Kristof van Laerhoven and Bernt Schiele. 2010. Coming to grips with the objects we grasp: detecting interactions with efficient wrist-worn sensors. In *Proceedings of the fourth international conference on Tangible, embedded, and embodied interaction* (TEI'10), 57-64. DOI=http://dx.doi.org/10.1145/1709886.1709898

[3]   Michael Boyle and Saul Greenberg. 2005. The language of privacy: Learning from video media space analysis and design. *ACM Trans. Comput.-Hum. Interact.*, 12 (2). 328-370. DOI= http://dx.doi.org /10.1145/1067860.1067868

[4]   Leah Buechley and Michael Eisenberg. 2009. Fabric PCBs, electronic sequins, and socket buttons: techniques for e-textile craft. *Personal Ubiquitous Comput.*, 13 (2). 133-150. DOI=https://doi.org/10.1007/s00779-007-0181-0

[5]   Michael Buettner, Richa Prasad, Matthai Philipose and David Wetherall. 2009. Recognizing daily activities with RFID-based sensors. In *Proceedings of the 11th international conference on Ubiquitous computing* (UbiComp'09), 51-60. DOI=http://doi.acm.org/10.1145/1620545.1620553

[6]   Perumal Varun Chadalavada, Goutham Palaniappan, Vimal Kumar Chandran, Khai Truong and Daniel Wigdor. 2018. ID'em: Inductive Sensing for Embedding and Extracting Information in Robust Materials. In *Proceedings of the ACM on Interactive, Mobile, Wearable and Ubiquitous Technologies*, 2 (3). 1-28. DOI=https://doi.org/10.1145/3264907

[7]   Liwei Chan, Yi-Ling Chen, Chi-Hao Hsieh, Rong-Hao Liang and Bing-Yu Chen. 2015. CyclopsRing: Enabling Whole-Hand and Context-Aware

Interactions Through a Fisheye Ring. In *Proceedings of the 28th Annual ACM Symposium on User Interface Software and Technology*, 549-556.
DOI=https://doi.org/10.1145/2807442.2807450

[8] Kai-Yin Cheng, Rong-Hao Liang, Bing-Yu Chen, Rung-Huei Laing and Sy-Yen Kuo. 2010. iCon: utilizing everyday objects as additional, auxiliary and instant tabletop controllers. In *Proceedings of the SIGCHI Conference on Human Factors in Computing Systems* (CHI'10), 1155-1164.
DOI=https://doi.org/10.1145/1753326.1753499

[9] Kunigunde Cherenack, Christoph Zysset, Thomas Kinkeldei, Niko Münzenrieder and Gerhard Tröster. 2010. Woven Electronic Fibers with Sensing and Display Functions for Smart Textiles. *Advanced Materials*, 22 (45). 5178-5182.
DOI=https://doi.org/10.1002/adma.201002159

[10] Lucy E. Dunne, Kaila Bibeau, Lucie Mulligan, Ashton Frith and Cory Simon. 2012. Multi-layer e-textile circuits. In *Proceedings of the 2012 ACM Conference on Ubiquitous Computing* (UbiComp'12), 649-650.
DOI=http://dx.doi.org/10.1145/2370216.2370348

[11] Jun Gong, Xin Yang, Teddy Seyed, Josh Urban Davis and Xing-Dong Yang. 2018. Indutivo: Contact-Based, Object-Driven Interactions with Inductive Sensing. In *Proceedings of the 31st Annual ACM Symposium on User Interface Software and Technology* (UIST'18), 321-333.
DOI=https://doi.org/10.1145/3242587.3242662

[12] Tobias Grosse-Puppendahl, Sebastian Herber, Raphael Wimmer, Frank Englert, Sebastian Beck, Julian von Wilmsdorff, Reiner Wichert and Arjan Kuijper. 2014. Capacitive near-field communication for ubiquitous interaction and perception. In *Proceedings of the 2014 ACM International Joint Conference on Pervasive and Ubiquitous Computing* (UbiComp'14), 231-242.
DOI=https://doi.org/10.1145/2632048.2632053

[13] Sunao Hashimoto, Ryohei Suzuki, Youichi Kamiyama, Masahiko Inami and Takeo Igarashi. 2013. LightCloth: senseable illuminating optical fiber cloth for creating interactive surfaces. In *CHI '13 Extended Abstracts on Human Factors in Computing Systems* (CHI EA'13), 2809-2810.
DOI=https://doi.org/10.1145/2468356.2479523

[14] Gerard J. Hayes, Ying Liu, Jan Genzer, Gianluca Lazzi and Michael D. Dickey. 2014. Self-Folding Origami Microstrip Antennas. *IEEE Transactions on Antennas and Propagation*, 62 (10). 5416-5419.
DOI=https://doi.org/10.1109/TAP.2014.2346188

[15] Steve Hodges, Alan Thorne, Hugo Mallinson and Christian Floerkemeier. 2007. Assessing and optimizing the range of UHF RFID to enable real-world pervasive computing applications. In *International Conference on Pervasive Computing*, 280-297.
DOI=https://doi.org/10.1007/978-3-540-72037-9_17

[16] David I Lehn, Craig W Neely, Kevin Schoonover, Thomas L Martin and Mark Jones. 2004. e-TAGs: e-textile attached gadgets. In *Proceedings of the Communication Networks and Distributed Systems Modeling and Simulation Conference.*

[17] Hiren Galiyawala Kinjal H. Pandya. 2014. A Survey on QR Codes : in context of Research and Application. *International Journal of Emerging Technology and Advanced Engineering.* 4 (3). 258-262.

[18] Gierad Laput, Robert Xiao and Chris Harrison. 2016. Viband: High-fidelity bio-acoustic sensing using commodity smartwatch accelerometers. In *Proceedings of the 29th Annual Symposium on User Interface Software and Technology* (UIST'16), 321-333.
DOI=https://doi.org/10.1145/2984511.2984582

[19] Gierad Laput, Chouchang Yang, Robert Xiao, Alanson Sample and Chris Harrison. 2015. Em-sense: Touch recognition of uninstrumented, electrical and electromechanical objects. In *Proceedings of the 28th Annual ACM Symposium on User Interface Software and Technology* (UIST'15), 157-166.
DOI=https://doi.org/10.1145/2807442.2807481

[20] Joanne Leong, Patrick Parzer, Florian Perteneder, Teo Babic, Christian Rendl, Anita Vogl, Hubert Egger, Alex Olwal and Michael Haller. 2016. proCover: Sensory Augmentation of Prosthetic Limbs Using Smart Textile Covers. In *Proceedings of the 29th Annual Symposium on User Interface Software and Technology* (UIST'16), 335-346.
DOI=https://doi.org/10.1145/2984511.2984572

[21] Hanchuan Li, Eric Brockmeyer, Elizabeth J. Carter, Josh Fromm, Scott E. Hudson, Shwetak N. Patel and Alanson Sample. 2016. PaperID: A Technique for Drawing Functional Battery-Free Wireless Interfaces on Paper. In *Proceedings of the 2016 CHI Conference on Human Factors in Computing Systems* (CHI'16)*, 5885-5896.
DOI=https://doi.org/10.1145/2858036.2858249

[22] Hanchuan Li, Can Ye and Alanson P. Sample. 2015. IDSense: A Human Object Interaction Detection System Based on Passive UHF RFID. In *Proceedings of the 33rd Annual ACM Conference on Human Factors in Computing Systems* (CHI'15), 2555-2564.
DOI=https://doi.org/10.1145/2702123.2702178

[23] Jaime Lien, Nicholas Gillian, M. Emre Karagozler, Patrick Amihood, Carsten Schwesig, Erik Olson, Hakim Raja and Ivan Poupyrev. 2016. Soli: Ubiquitous Gesture Sensing with Millimeter Wave Radar. In *ACM Transactions on Graphics* (SIGGRAPH'16).
DOI=https://doi.org/10.1145/2897824.2925953

[24] David G. Lowe. 1999. Object recognition from local scale-invariant features. In *Proceedings of the Seventh*

IEEE International Conference on Computer Vision (ICCV'99), 1150-1157.
DOI=https://doi.org/10.1109/ICCV.1999.790410

[25] Takuya Maekawa, Yasue Kishino, Yutaka Yanagisawa and Yasushi Sakurai. 2012. Recognizing handheld electrical device usage with hand-worn coil of wire. In *International Conference on Pervasive Computing* (Pervasive'12), 234-252.
DOI=https://doi.org/10.1007/978-3-642-31205-2_15

[26] Jan Meyer, Bert Arnrich, Johannes Schumm and Gerhard Troster. 2010. Design and Modeling of a Textile Pressure Sensor for Sitting Posture Classification. *IEEE Sensors Journal*, 10 (8). 1391-1398.
DOI=https://doi.org/10.1109/JSEN.2009.2037330

[27] Norhisam Misron, Loo Qian Ying, Raja Nor Firdaus, Norrimah Abdullah, Nashiren Farzilah Mailah and Hiroyuki Wakiwaka. 2011. Effect of inductive coil shape on sensing performance of linear displacement sensor using thin inductive coil and pattern guide. *Sensors*, 11 (11). 10522-10533.
DOI=https://doi.org/10.3390/s111110522

[28] Sunderarajan S Mohan, Maria del Mar Hershenson, Stephen P Boyd and Thomas H Lee. 1999. Simple accurate expressions for planar spiral inductances. *IEEE Journal of solid-state circuits*, 34 (10). 1419-1424.
DOI=https://doi.org/10.1109/4.792620

[29] David S. Nyce. Inductive Sensing. In *Linear Position Sensors*. 78–93.
DOI=https://doi.org/10.1002/0471474282

[30] Patrick Parzer, Florian Perteneder, Kathrin Probst, Christian Rendl, Joanne Leong, Sarah Schuetz, Anita Vogl, Reinhard Schwoediauer, Martin Kaltenbrunner, Siegfried Bauer and Michael Haller. 2018. RESi: A Highly Flexible, Pressure-Sensitive, Imperceptible Textile Interface Based on Resistive Yarns. In *Proceedings of the 31st Annual ACM Symposium on User Interface Software and Technology* (UIST'18), 745-756.
DOI=https://doi.org/10.1145/3242587.3242664

[31] Patrick Parzer, Kathrin Probst, Teo Babic, Christian Rendl, Anita Vogl, Alex Olwal and Michael Haller. 2016. FlexTiles: A Flexible, Stretchable, Formable, Pressure-Sensitive, Tactile Input Sensor. In *Proceedings of the 2016 CHI Conference Extended Abstracts on Human Factors in Computing Systems* (CHI EA'16), 3754-3757.
DOI=https://doi.org/10.1145/2851581.2890253

[32] Patrick Parzer, Adwait Sharma, Anita Vogl, Jurgen Steimle, Alex Olwal and Michael Haller. 2017. SmartSleeve: Real-time Sensing of Surface and Deformation Gestures on Flexible, Interactive Textiles, using a Hybrid Gesture Detection Pipeline. In *Proceedings of the 30th Annual ACM Symposium on User Interface Software and Technology* (UIST'17), 565-577.

[33] Vesa Peltonen, Juha Tuomi, Anssi Klapuri, Jyri Huopaniemi and Timo Sorsa. 2002. Computational auditory scene recognition. In *IEEE International Conference on Acoustics, Speech, and Signal Processing* (ICASSP'02), II-1941-II-1944.
DOI=https://doi.org/10.1109/ICASSP.2002.5745009

[34] Alex "Sandy" Pentland. 1998. Wearable Intelligence. *Scientific American*, 90-95.

[35] Ivan Poupyrev, Nan-Wei Gong, Shiho Fukuhara, Mustafa Emre Karagozler, Carsten Schwesig and Karen E. Robinson. 2016. Project Jacquard: Interactive Digital Textiles at Scale. In *Proceedings of the 2016 CHI Conference on Human Factors in Computing Systems* (CHI'16), 4216-4227.
DOI=https://doi.org/10.1145/2858036.2858176

[36] Juhi Ranjan, Yu Yao, Erin Griffiths and Kamin Whitehouse. 2012. Using mid-range RFID for location based activity recognition. In *Proceedings of the 2012 ACM Conference on Ubiquitous Computing* (UbiComp'12), 647-648.
DOI=http://dx.doi.org/10.1145/2370216.2370347

[37] Mahsan Rofouei, Wenyao Xu and Majid Sarrafzadeh. 2010. Computing with uncertainty in a smart textile surface for object recognition. In *2010 IEEE Conference on Multisensor Fusion and Integration*, 174-179.
DOI=http://dx.doi.org/10.1109/MFI.2010.5604473

[38] Edward B. Rosa. 1906. Calculation of the self-inductances of single-layer coils. *Bull. Bureau Standards*, 2 (2). 161-187.

[39] Edward Bennett Rosa. 1908. The self and mutual inductances of linear conductors.

[40] Stefan Schneegass and Alexandra Voit. 2016. GestureSleeve: using touch sensitive fabrics for gestural input on the forearm for controlling smartwatches. In *Proceedings of the 2016 ACM International Symposium on Wearable Computers* (ISWC '16), 108-115.
DOI=https://doi.org/10.1145/2971763.2971797

[41] Jamie Shotton, Andrew Fitzgibbon, Mat Cook, Toby Sharp, Mark Finocchio, Richard Moore, Alex Kipman and Andrew Blake. 2011. Real-time human pose recognition in parts from single depth images. In *Conference on Computer Vision and Pattern Recognition* (CVPR'11), 1297-1304.
DOI=https://doi.org/10.1109/CVPR.2011.5995316

[42] Joshua R Smith, Kenneth P Fishkin, Bing Jiang, Alexander Mamishev, Matthai Philipose, Adam D Rea, Sumit Roy and Kishore Sundara-Rajan. 2005. RFID-based techniques for human-activity detection. *Communications of the ACM*, 48 (9). 39-44.
DOI=http://dx.doi.org/10.1145/1081992.1082018

[43] Jie Song, Gábor Sörös, Fabrizio Pece, Sean Ryan Fanello, Shahram Izadi, Cem Keskin, and Otmar Hilliges. 2014. In-air gestures around unmodified mobile devices. In *Proceedings of the 27th annual*

ACM symposium on User interface software and technology (UIST '14), 319-329.
DOI=https://doi.org/10.1145/2642918.2647373

[44] Michael E. Van Steenberg, Andrew Washabaugh, and Neil Goldfme. 2001. Inductive and capacitive sensor arrays for in situ composition sensors. In *Proceedings of 2001 IEEE Aerospace Conference.*
DOI=https://doi.org/10.1109/AERO.2001.931721

[45] Yuta Sugiura, Gota Kakehi, Anusha Withana, Calista Lee, Daisuke Sakamoto, Maki Sugimoto, Masahiko Inami and Takeo Igarashi. 2011. Detecting shape deformation of soft objects using directional photoreflectivity measurement. In *Proceedings of the 24th annual ACM symposium on User interface software and technology* (UIST'11), 509-516.
DOI=https://doi.org/10.1145/2047196.2047263

[46] Nalika Ulapane, Linh Nguyen, Jaime Valls Miro, Alen Alempijevic and Gamini Dissanayake. 2017. Designing a pulsed eddy current sensing set-up for cast iron thickness assessment. In *12th IEEE Conference on Industrial Electronics and Applications (ICIEA'17)*, 901-906.
DOI=https://doi.org/10.1109/ICIEA.2017.8282967

[47] Nicolas Villar, Daniel Cletheroe, Greg Saul, Christian Holz, Tim Regan, Oscar Salandin, Misha Sra, Hui-Shyong Yeo, William Field and Haiyan Zhang. 2018. Project Zanzibar: A Portable and Flexible Tangible Interaction Platform. In *Proceedings of the 2018 CHI Conference on Human Factors in Computing Systems.*
DOI=https://doi.org/10.1145/3173574.3174089

[48] Anita Vogl, Patrick Parzer, Teo Babic, Joanne Leong, Alex Olwal and Michael Haller. 2017. StretchEBand: Enabling Fabric-based Interactions through Rapid Fabrication of Textile Stretch Sensors. In *Proceedings of the 2017 CHI Conference on Human Factors in Computing Systems* (CHI'17), 2617-2627.
DOI=https://doi.org/10.1145/3025453.3025938

[49] Edward J Wang, Tien-Jui Lee, Alex Mariakakis, Mayank Goel, Sidhant Gupta and Shwetak N Patel. 2015. Magnifisense: Inferring device interaction using wrist-worn passive magneto-inductive sensors. In *Proceedings of the 2015 ACM International Joint Conference on Pervasive and Ubiquitous Computing* (UbiComp'15), 15-26.
DOI=https://doi.org/10.1145/2750858.2804271

[50] Jamie A Ward, Paul Lukowicz, Gerhard Troster and Thad E Starner. 2006. Activity recognition of assembly tasks using body-worn microphones and accelerometers. *IEEE transactions on pattern analysis and machine intelligence*, 28 (10). 1553-1567.
DOI=https://doi.org/10.1109/TPAMI.2006.197

[51] Robert Xiao, Gierad Laput, Yang Zhang and Chris Harrison. 2017. Deus EM Machina: on-touch contextual functionality for smart IoT appliances. In *Proceedings of the 2017 CHI Conference on Human Factors in Computing Systems* (CHI'17), 4000-4008.
DOI=https://doi.org/10.1145/3025453.3025828

[52] Wenyao Xu, Ming-Chun Huang, Navid Amini, Lei He and Majid Sarrafzadeh. 2013. eCushion: A Textile Pressure Sensor Array Design and Calibration for Sitting Posture Analysis. *IEEE Sensors Journal*, 13 (10). 3926-3934.
DOI=https://doi.org/10.1109/JSEN.2013.2259589

[53] Hui-Shyong Yeo, Gergely Flamich, Patrick Schrempf, David Harris-Birtill and Aaron Quigley. 2016. Radarcat: Radar categorization for input and interaction. In *Proceedings of the 29th Annual Symposium on User Interface Software and Technology* (UIST'16), 833-841.
DOI=https://doi.org/10.1145/2984511.2984515

[54] Jonsenser Zhao. 2010. A new calculation for designing multilayer planar spiral inductors. EDN (Electrical Design News), 55 (14). 37.